Supplemental Information for: “A Systematic Resolution of Sulfur in Reticulated Vitreous Carbon Using X-ray Absorption Spectroscopy” by Patrick Frank, Serena DeBeer George, Elodie Anxolabéhère-Mallart, Britt Hedman, and Keith O. Hodgson.

Supplemental Figure 1

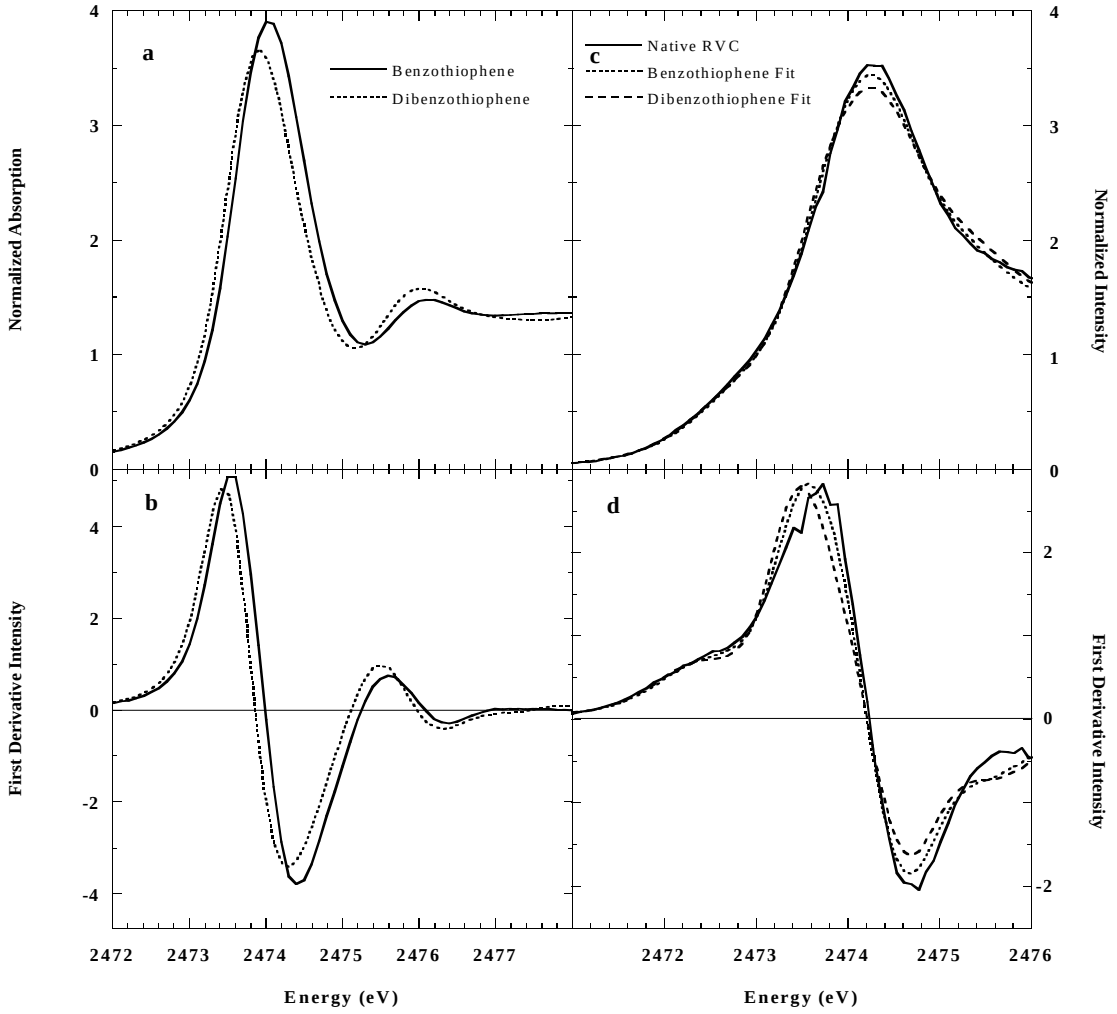

Figures S1a and S1b: Comparison of the rising edge energy region of the sulfur K-edge spectrum of benzothiophene and of dibenzothiophene. The rising edge maxima differ by about 0.1 eV but the overall shapes of the XAS spectra are similar, as expected from the similarity of the respective molecular structures. Figures S1c and S1d compare otherwise equivalent fits to the low-energy region of the sulfur K-edge XAS of native RVC on exchange of benzothiophene and dibenzothiophene. The component fractions were 0.237 and 0.244, respectively, and the goodness-of-fit ‘F’-values were 0.33×10^{-2} and 0.37×10^{-2}. This result illustrates the sensitivity of XAS edge spectral fits to relatively small variations in the structure of models having otherwise identical sulfur functional groups.

Supplemental Figure 2

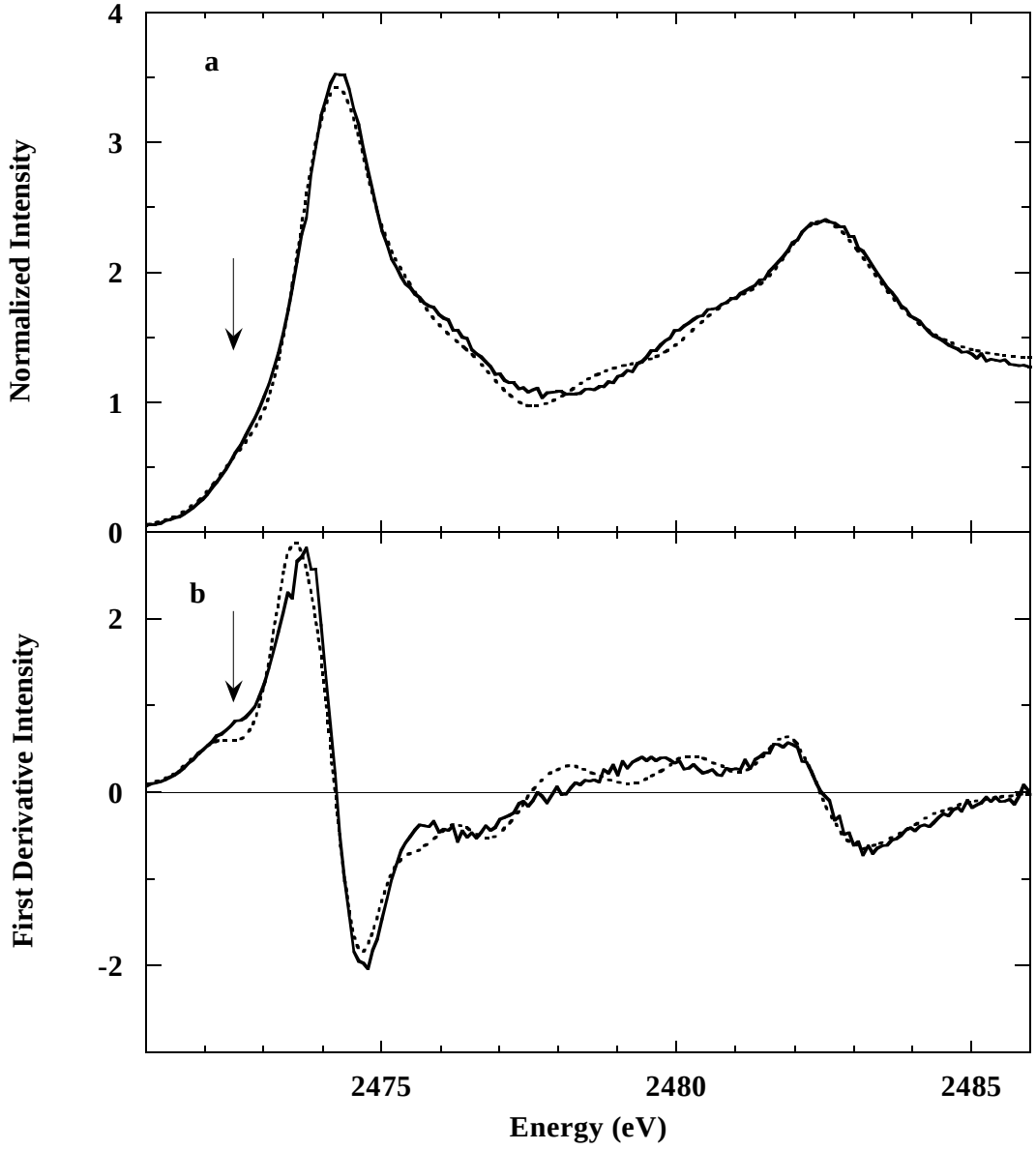

Figure S2: a. (—), Sulfur K-edge XAS spectrum of native RVC, and; (···), the best fit to the RVC sulfur K-edge XAS spectrum obtained without including the sulfur K-edge XAS spectrum of ethylene episulfide. b. The first derivative sulfur K-edge spectra of part 'a.' Arrows mark the energy region left unfit without inclusion of the episulfide XAS model.

Supplemental Figure 3

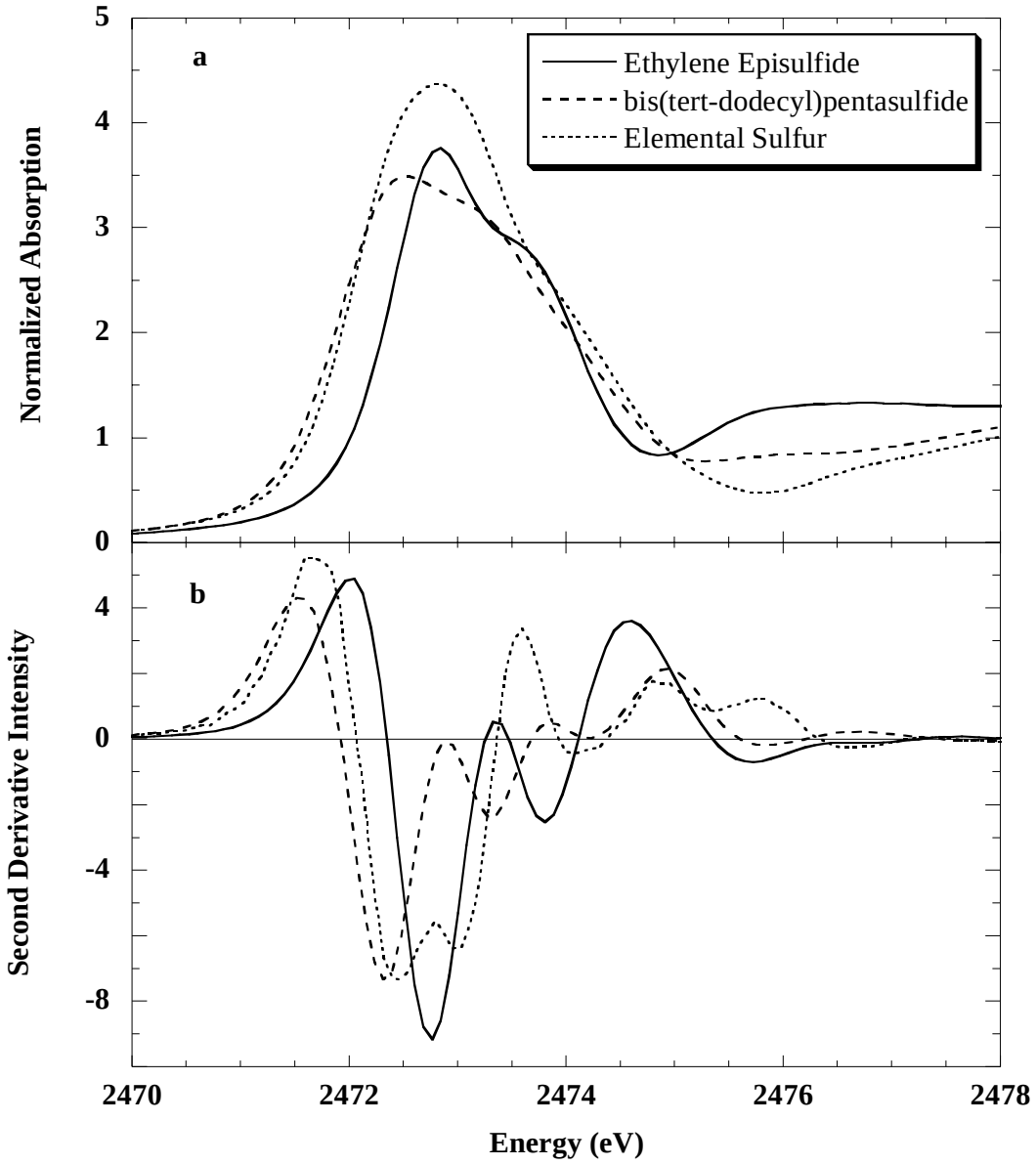

Figure S3: The normalized sulfur K-edge XAS spectra (top) and the second derivatives of the XAS spectra (bottom) of ethylene episulfide, of bis(tert-dodecyl)pentasulfide, and of elemental sulfur, all ≤0.1 M in sulfur in p-xylene solution.

Supplemental Figure 4

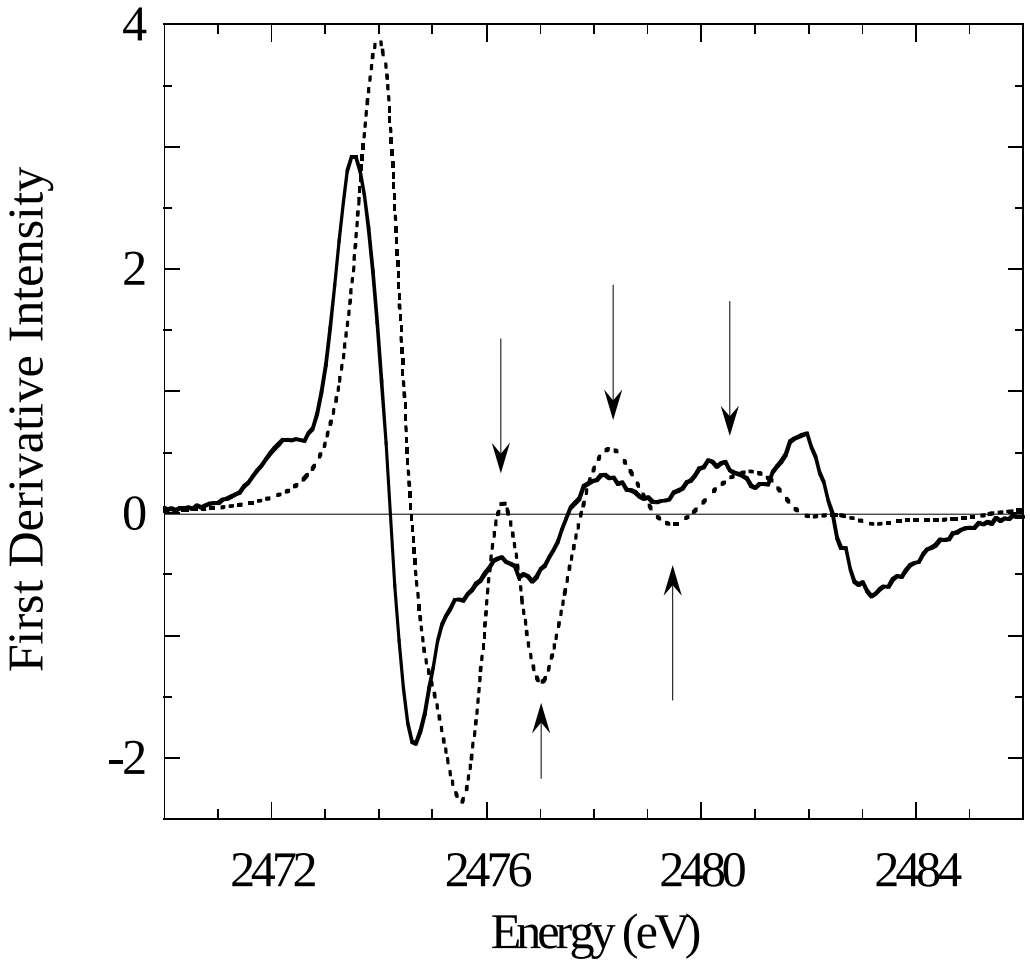

Figure S4: The first derivative sulfur K-edge XAS spectrum of: (—), the fit to native RVC, and; (···), N,N'-thiobisphthalimide. The strong but extraneous first derivative transition features that the sulfur K-edge XAS spectrum of N,N'-thiobisphthalimide contributed to the fit are indicated by arrows.

Derivation of the thermodynamic reaction model for sulfur in RVC

Let any sulfur-reactive sites in hot RVC be represented as α, β, χ, …, ζ, with the respective populations A_α, B_β, C_χ, …, Z_ζ. Assume these sites are Latent in cold RVC as A^L_α, B^L_β, …, Z^L_ζ, and are activated at pyrolysis temperatures (~1000 ºC) where they enter a thermal equilibrium, producing their active congener within the RVC carbon framework. Then the appearance of sulfur-reactive sites will be governed by the equilibrium relationships as in equations 1. Reactions 1 are assumed to lie far to the right under pyrolysis conditions:

$$\begin{aligned} A^L_\alpha &\rightleftharpoons A_\alpha & \frac{A_\alpha}{A^L_\alpha} &= e^{\frac{-\Delta G_\alpha}{RT}} \\ B^L_\beta &\rightleftharpoons B_\beta & & \\ C^L_\chi &\rightleftharpoons C_\chi & \vdots & \\ Z^L_\zeta &\rightleftharpoons Z_\zeta & \frac{Z_\zeta}{Z^L_\zeta} &= e^{\frac{-\Delta G_\zeta}{RT}} \end{aligned} \qquad \textbf{S1}$$

The population of each sulfur-reactive site, A_α, B_β, etc., normalized to the mass of RVC, e.g., $A_\alpha/(RVC)_{mass}$, is equivalent to an equilibrium concentration, $[\alpha]_t$, $[\beta]_t$, etc., where subscript 't' represents the 'total' concentration of active sites 'α,' 'β,' etc. The equilibrium concentrations $[\alpha]_t$, $[\beta]_t$ …, etc., will be constants at a given temperature to the extent that RVC averages to a uniform matrix. At equilibrium a minority sulfur population will partition itself among these sites as aS_α, bS_β, cS_χ, …, zS_ζ, where *a*, *b*, *c*,…, *z* are occupancies and S_α, S_β,… represent sulfur atoms in RVC sites α, β, ... Then, e.g., (aS_α/A_α) represents the fractional proportion of alpha-type sites occupied by sulfur, and $[(S_{at.\ wt.})\times(aS_\alpha+bS_\beta+cS_\chi+ \dots +zS_\zeta)]/(\text{RVC mass}) = [S]_{total}$ (in, e.g., ppm). If this

simple analysis holds, then the partitioning of sulfur into sites α, β, χ, ..., ζ in RVC can be described by the equilibrium equations 2, where the subscript 'f' refers to free reactant.

$$\mathbf{S + \alpha \rightleftharpoons S_\alpha \qquad K_\alpha = [S_\alpha]/[S]_f[\alpha]_f}$$
$$\mathbf{S + \beta \rightleftharpoons S_\beta \qquad K_\beta = [S_\beta]/[S]_f[\beta]_f} \qquad \textbf{S2}$$
$$\vdots$$

For different batches of RVC across all the production-standard pyrolytic runs for which $[S]_{total}$ is small and similar, and for which A, B, C » a, b, c, and $[\alpha]_t+[\beta]_t+[\chi]_t+ \ldots +[\zeta]_t >> [S]_{total}$, the decrease in concentration from the initial $[\alpha]_t$, $[\beta]_t$, …, etc., will be small following the equilibrium reaction with sulfur. In this case the approximation $[\alpha]_f \approx [\alpha]_t$, $[\beta]_f \approx [\beta]_t$, etc., should hold and all the equations 2 can be re-written as, e.g.,

$$\mathbf{[S_\alpha] = K_\alpha \times [S]_f \times [\alpha]_t}$$
$$\mathbf{[S_\beta] = K_\beta \times [S]_f \times [\beta]_t} \qquad \textbf{S3}$$
$$\vdots$$

In this form, plots of $[S]_f$ vs. $[S_\alpha]$, $[S_\beta]$, …, obtainable from sulfur K-edge XAS fits, will be a series of straight lines passing through 0,0, of slope $K_\alpha \times [\alpha]_t$, …, etc. The ratios of $[S_\alpha]:[S_\beta]:[S_\chi]: \ldots :[S_\zeta]$ will be constants equal to the ratios of the slopes of the lines. Likewise, from the mass-balance and equations 3, we can write: Total sulfur, $[S]_t = [S]_f+[S_\alpha]+[S_\beta]+\ldots+[S_\zeta] = [S]_f+\{[S]_f \times K_\alpha \times [\alpha]_t\}+\{[S]_f \times K_\beta \times [\beta]_t\}+\ldots+\{[S]_f \times K_\zeta \times [\zeta]_t\}$, and $[S]_t = [S]_f \times [1+\text{constant}]$. Thus $[S]_t$ will follow the same linearity as $[S]_f$ in the above analysis, and the fractional percents of each sulfur type, $([S_\alpha]/[S]_t):([S_\beta]/[S]_t)$, etc., will be constant ratios. It follows, then, that the fractional proportion of, e.g., S_α in RVC =

$(S_{at.wt} \times aS_{\alpha}/A_{\alpha}) \times (A_{\alpha}/RVC_{mass}) = (S_{\alpha})_{mass}/(RVC)_{mass}$ will vary almost linearly with total sulfur for all RVC prepared under the same equilibrium pyrolysis conditions, so long as $[S]_t$ is small relative to the concentration of reactive carbon sites.

Within the above linear limit, when the total sulfur is normalized to 100%, the distribution of sulfur functional groups in different production batches of RVC can be directly compared because the relative proportions of sulfur types should follow linear slopes. The success of this analysis would invite further characterization of sulfur sites in RVC. For example, knowledge of $[S]_f$ and $[S_{\alpha}]$, $[S_{\beta}]$, etc., from fits to the sulfur K-edge XAS data of a series of RVC samples of varying sulfur concentration, would allow a Scatchard formalism analysis[Dahlquist, 1978 #338] for each sulfur binding site, as exemplified in equation 4 for the α-type sites:

$$\frac{[S_{\alpha}]}{[S]_f} = K_{\alpha}([\alpha]_t - [S_{\alpha}]) \qquad \textbf{S4}$$

A plot of $[S_{\alpha}]/[S]_f$ vs. $[S_{\alpha}]$, should then yield K_{α} from the slope and $[\alpha]_t$ from the intercept, providing a full exposition of reactions 3. The quantity $[\alpha]_t$ is equivalent to the A_{α} of equation 1, and an Arrhenius study then applied as equations 1 could yield the formational thermodynamics of each sulfur reactive RVC site from its latent site.